All-Orders Quadratic-Logarithmic Behavior for Amplitudes

Benjamin Basso,[1,*] Lance J. Dixon,[2,†] Yu-Ting Liu,[2,3,‡] and Georgios Papathanasiou[4,§]
[1]Laboratoire de Physique de l'Ecole Normale Supérieure, ENS, Université PSL, CNRS, Sorbonne Université, Université Paris Cité, F-75005 Paris, France
[2]SLAC National Accelerator Laboratory, Stanford University, Stanford, California 94309, USA
[3]Kavli Institute for Theoretical Physics, UC Santa Barbara, Santa Barbara, California 93106, USA
[4]Deutsches Elektronen-Synchrotron DESY, Notkestraße 85, 22607 Hamburg, Germany

(Received 1 December 2022; accepted 9 February 2023; published 16 March 2023)

We classify origin limits of maximally helicity violating multigluon scattering amplitudes in planar $\mathcal{N}=4$ super-Yang-Mills theory, where a large number of cross ratios approach zero, with the help of cluster algebras. By analyzing existing perturbative data and bootstrapping new data, we provide evidence that the amplitudes become the exponential of a quadratic polynomial in the large logarithms. With additional input from the thermodynamic Bethe ansatz at strong coupling, we conjecture exact expressions for amplitudes with up to eight gluons in all origin limits. Our expressions are governed by the tilted cusp anomalous dimension evaluated at various values of the tilt angle.

DOI: 10.1103/PhysRevLett.130.111602

Introduction.—For generic kinematics, perturbative scattering amplitudes can be extremely complicated functions of the kinematic variables. In certain limits, they may simplify enormously. For general gauge theories, simplifying kinematics include Sudakov regions, where soft gluon radiation is suppressed, and high-energy or multi-Regge limits, where Regge factorization holds. In planar $\mathcal{N}=4$ super-Yang-Mills theory (SYM), the duality of amplitudes to polygonal Wilson loops [1–4] allows near-collinear limits to be computed [5,6] in terms of excitations of the Gubser-Klebanov-Polyakov flux tube [7,8]. Recently, an even simpler kinematical region for six-gluon scattering in the maximally helicity-violating (MHV) configuration was found [9,10], the "origin" where all three cross ratios of the dual hexagon Wilson loop are sent to zero. In this limit, the logarithm of the MHV amplitude becomes quadratic in the logarithms of the cross ratios. The coefficients of the two quadratic polynomials, $\Gamma_{\rm oct}$ and $\Gamma_{\rm hex}$, can be computed for any value of the 't Hooft coupling $\lambda \equiv g^2/(16\pi^2)$ by deforming the Beisert-Eden-Staudacher (BES) kernel [11] by a "tilt" angle α, giving rise to a "tilted cusp anomalous dimension" $\Gamma_\alpha(g)$ (see Sec. A of the Supplemental Material [12]). The usual Beisert-Eden-Staudacher kernel and cusp anomalous dimension are recovered by setting $\alpha=\pi/4$, $\Gamma_{\rm cusp}=\Gamma_{\alpha=\pi/4}$, while the two hexagon-origin coefficients are given by $\Gamma_{\rm oct}=\Gamma_{\alpha=0}$ and $\Gamma_{\rm hex}=\Gamma_{\alpha=\pi/3}$.

This Letter will explore analogous origins for higher-point MHV amplitudes, regions where the same quadratic logarithmic (QL) behavior holds. We will see that there is a cornucopia of such regions at seven and especially eight points. The regions need not be isolated points; they can be one-dimensional lines starting at seven points, and up to three-dimensional surfaces starting at eight points. They can be classified by cluster algebras [16,17], which provide natural compactifications of the space of positive kinematics [18–21], at the boundary of which these limits are located. Furthermore, we will provide a master formula that we conjecture organizes the QL behavior of MHV amplitudes in all of these regions for arbitrary coupling, as a discrete sum over tilt angles, in which $\Gamma_\alpha(g)$ carries all of the coupling dependence. Our formula is motivated by studying the thermodynamic Bethe ansatz (TBA) representation [5,22–24] of the minimal-area formula [1] for the amplitude at strong coupling.

Classifying origin limits.—Dual conformal symmetry [1–4,25] in planar $\mathcal{N}=4$ SYM implies that MHV amplitudes for n gluons depend on $3(n-5)$ independent kinematical variables. These may be chosen as a subset of the $n(n-5)/2$ dual conformal cross ratios,

$$u_{i,j}=\frac{x^2_{i,j+1}x^2_{j,i+1}}{x^2_{i,j}x^2_{j+1,i+1}}, \tag{1}$$

where $x^\mu_{i,j}\equiv p^\mu_i+p^\mu_{i+1}+\cdots+p^\mu_{j-1}$ are sums of cyclicly adjacent gluon momenta, and indices are always mod n.

For $n=6$, all cross ratios $u_i\equiv u_{i+1,i+4}$, $i=1,2,3$ are independent, and the origin limit is simply defined as the kinematic point

$$\mathrm{O}^{(6)}\colon\ u_i \to 0, \quad i = 1,2,3. \tag{2}$$

At higher n, there are $(n-5)(n-6)/2$ Gram determinant polynomial relations between the cross ratios, because there are a limited number of independent vectors in fixed spacetime dimensions. (For their explicit form for $n = 7, 8$, see Sec. B of the Supplemental Material [12].) These relations raise the question of how to define the appropriate generalizations of the origin limit.

To answer this question, we consider the "positive region," a subregion of Euclidean scattering kinematics where amplitudes are expected to be devoid of branch points [19,26]. Thus, the first place to look for simple divergent behavior is at pointlike limits at the boundary of the positive region. Such limits may be found systematically using "cluster algebras" [16,17] associated with the Grassmannian $\mathrm{Gr}(4,n)$ [27], which provide a compactification of the positive region [18–21]; see also [28]. Accordingly, the positive region may be mapped to the inside of a polytope, whose boundary comprises vertices connected by edges that bound polygonal faces, that bound higher-dimensional polyhedra. Cluster algebras, or more precisely cluster Poisson varieties, consist of a collection of clusters, each containing $3(n-5)$ cluster $\mathcal{X}$-coordinates $\mathcal{X}_i$, corresponding to a coordinate chart describing this compactification. Setting all $\mathcal{X}_i \to 0$ yields a vertex at the boundary of the positive region. Letting all but one $\mathcal{X}_i$ vanish gives an edge connecting neighboring clusters, known as a "mutation." It is also associated with a birational transformation between the $\mathcal{X}$ coordinates of the connected clusters, enabling the generation of a cluster algebra from an initial cluster.

We start with the finite $\mathrm{Gr}(4,n)$ cluster algebras for $n = 6$, 7, with Dynkin labels A_3 and E_6 [17]. We first observe that in all boundary vertices $u_{i,j} = 0$ or 1. These kinematic points contain the $n = 6$ origin limit, Eq. (2); at $n = 7$ we find 28 clusters describing analogous limits where all but one of the seven $u_i \equiv u_{i+1,i+4}$, $i = 1,2,\ldots,7$ vanishes,

$$\mathrm{O}_j^{(7)}\colon\ u_{i\neq j} \to 0, \qquad u_j = 1. \tag{3}$$

The seven origins are related by a cyclic symmetry, $u_i \mapsto u_{i+1}$. There are four clusters for each $\mathrm{O}_j^{(7)}$, two with a different direction of approach to the limit, plus their parity images.

All of these clusters form a cyclic chain connected by mutations or lines in the space of kinematics. In terms of cross ratios, the line connecting $\mathrm{O}_7^{(7)}$ and $\mathrm{O}_1^{(7)}$ is

$$\textsc{line}\,71\colon\ u_i \ll 1,\ \ i = 2,3,4,5,6; \quad u_7 + u_1 = 1, \tag{4}$$

with $u_1, u_7 \in [0,1]$. The remaining lines are obtained by cyclic symmetry. Quite remarkably, the amplitude exhibits exponentiated QL behavior not only on the points, Eq. (3), but also on these origin lines! This QL behavior also implies that the value of the amplitude is independent of the direction or speed of approach to the limit; it remains the same function of the cross ratios irrespective of the rate with which they tend to zero.

Inspired by these examples, we define "origin points" at higher n as vertices where at least $3(n-5)$ cross ratios approach zero. We now classify the $n = 8$ origin points. While the corresponding $\mathrm{Gr}(4,8)$ cluster algebra is infinite-dimensional, there is a procedure for selecting a finite subset of clusters [26,29–32] based on tropicalization [33]; see also [34]. Here, we start with a cluster corresponding to an origin point, and generate new clusters by mutations until this condition is no longer met. We find 1188 clusters contained in the finite subset selected in [26,29–32], as further described in Sec. C of the Supplemental Material [12] and in an ancillary file. Modding out by parity, dihedral symmetry, and direction of approach, these origins belong to the nine classes shown in Table I, where $u_i \equiv u_{i+1,i+4}$, $i = 1,2,\ldots,8$, and $v_i \equiv u_{i+1,i+5}$, $i = 1,2,3,4$. This table may be obtained even more simply by assuming that all cross ratios approach 0 or 1, and scanning for all combinations that satisfy the Gram determinant constraints. This process also identifies one more potential origin, $\mathrm{O_X} = (0,0,1,0,0,1,0,1;0,0,0,0)$, in the $(u_i;v_j)$ notation of Table I. It lies outside of the positive region, and we defer its study to future work.

At $n = 8$, there are also higher-dimensional QL surfaces connecting the O_i, which generalize the seven-point LINE 71, Eq. (4). Motivated by this line, which also defines an A_1 subalgebra of the E_6 cluster algebra, we searched for maximal subalgebras of the $\mathrm{Gr}(4,8)$ cluster algebra that move one solely from origin to origin. Two A_3 subalgebras correspond to two cubes, CUBE 6789 and CUBE 5678 [35]. Two A_2 subalgebras correspond to PENTAGON 345 and PENTAGON 234. An $A_1 \times A_1$ corresponds to SQUARE 456. An A_1 subalgebra SUPERLINE 1 connects two super-origins O_1. These high-dimensional spaces interpolating between origins are summarized in Table II and are depicted in Fig. 1.

TABLE I. All dihedrally inequivalent origin classes for $n = 8$. Zeros represent infinitesimal values. There are nine infinitesimal cross ratios for all origins except for the "super-origin" O_1, which has ten. All nonzero cross ratios are close to unity.

Origin class	u_1	u_2	u_3	u_4	u_5	u_6	u_7	u_8	v_1	v_2	v_3	v_4
O_1(super)	0	0	0	0	0	0	0	0	0	1	0	1
O_2	0	0	0	0	0	0	0	1	0	1	0	1
O_3	0	0	0	0	0	0	0	1	0	0	1	1
O_4	0	0	0	0	0	0	1	1	0	0	1	0
O_5	0	0	0	0	0	1	0	1	0	0	1	0
O_6	0	0	0	0	1	0	0	1	0	1	0	0
O_7	0	0	0	0	1	0	0	1	0	0	1	0
O_8	0	0	0	1	0	0	0	1	0	1	0	0
O_9	0	0	0	1	0	0	0	1	0	0	0	1

TABLE II. Relations among the finite cross ratios for the octagon boundaries. All the cross ratios unspecified in the relations are implicitly infinitesimal.

Boundary	Relations
CUBE 6789	$u_3+u_4=u_7+u_8=v_1+v_4=1$
CUBE 5678	$u_1+u_2=u_4+u_5=v_2+v_3=1$
SQUARE 456	$u_1+u_2=u_7+u_8=v_4=1$
PENTAGON 345	$u_8+u_1u_7=u_7+u_8v_4=v_4+u_7v_3=1$
PENTAGON 234	$u_1+u_8v_3=v_3+u_1v_4=u_8+u_1v_1=1$
SUPERLINE 1	$v_1=1-v_2=v_3=1-v_4$

Perturbative data and bootstrap.—In this Letter, we work with the n-point remainder function R_n, related to the MHV amplitude by

$$\exp R_n \equiv A_n^{\mathrm{MHV}}/A_n^{\mathrm{BDS}},$$

where the known, infrared-divergent normalization factor A_n^{BDS} is essentially the exponential of the one-loop amplitude [36–38]. The remainder function is infrared-finite and invariant under dual conformal symmetry as well as the n-gon dihedral symmetry group D_n.

Using perturbative data through seven loops, R_6 was found to simplify drastically [9] at the origin, Eq. (2): To $\mathcal{O}(u_i^0)$, it becomes the sum of two QL polynomials,

$$R_6=-\frac{\Gamma_0-\Gamma_{\pi/4}}{24}\ln^2(u_1u_2u_3)-\frac{\Gamma_{\pi/3}-\Gamma_{\pi/4}}{24}\sum_{i=1}^{3}\ln^2\left(\frac{u_i}{u_{i+1}}\right), \tag{5}$$

where each polynomial is multiplied by the tilted cusp anomalous dimension Γ_α evaluated at different angles $\alpha=0,\frac{\pi}{4},\frac{\pi}{3}$ [10]. For $n=6$, D_6 acts on the u_i as arbitrary S_3 permutations. The origin preserves this symmetry, so only S_3-symmetric quadratic polynomials are allowed, which are exhausted by those of Eq. (5).

For $n=7$, QL behavior was observed for R_7 through four loops at the dihedrally equivalent origins $\mathrm{O}_j^{(7)}$ [39]. More generally, a four-loop computation along the lines of Ref. [39] reveals that the remainder function R_7 on LINE 71, Eq. (4), is given by,

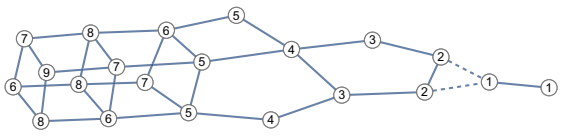

FIG. 1. The system of eight-point origins exhibiting QL behavior. We omit many origins that are related to the ones shown by dihedral symmetry. The node numbers correspond to O_i in Table I or their dihedral images. The behavior on the lines and surfaces shown in the figure is also QL, except for the dashed line between O_1 and O_2.

$$R_7(\text{LINE 71})=\sum_{i=1}^{3}c_iP_i^{(7)}, \tag{6}$$

where

$$\begin{aligned}P_1^{(7)}&=\sum_{i=1}^{6}l_il_{i+1}+\sum_{i=1}^{5}l_il_{i+2},\\ P_2^{(7)}&=-l_1l_7+\sum_{i=1}^{7}l_i^2+\sum_{i=1}^{4}l_il_{i+3},\\ P_3^{(7)}&=\sum_{i=1}^{7}l_il_{i+2}-\sum_{i=1}^{3}l_il_{i+4}\end{aligned} \tag{7}$$

are quadratic polynomials in the logarithms, $l_i\equiv\ln u_i$. In Eq. (6) and in the following, we give only the leading QL behavior in the given limit. We never find any linear-logarithmic terms. There are constant terms followed by subleading power corrections, which we do not study.

Through four loops, the coefficients c_i in Eq. (6) are given by

$$\begin{aligned}c_1&=g^4\zeta_2-\frac{37}{2}g^6\zeta_4+g^8\left(\frac{1975}{8}\zeta_6-2\zeta_3^2\right)+O(g^{10}),\\ c_2&=-\frac{5}{2}g^6\zeta_4+g^8\left(\frac{413}{8}\zeta_6-2\zeta_3^2\right)+O(g^{10}),\\ c_3&=-\frac{35}{8}g^8\zeta_6+O(g^{10}),\end{aligned} \tag{8}$$

where $\zeta_n=\sum_{k=1}^{\infty}k^{-n}$ is the Riemann zeta value.

We can derive the decomposition, Eq. (6), to all loop orders via a "baby" amplitude bootstrap, using the following conditions. (1) We assume that R_7 is QL. (2) Continuity—the result at $\mathrm{O}_7^{(7)}$ ($\mathrm{O}_1^{(7)}$) is obtained from that on LINE 71 by setting $l_7\to 0$ ($l_1\to 0$). (3) The following three conditions from dihedral symmetry: (i) The full D_7 is broken on the line but a single reflection (flip) survives: $u_i\leftrightarrow u_{8-i}$. It exchanges the two end points $u_7=1$ and $u_1=1$. (ii) There is a flip symmetry at $u_7=1$: $u_i\leftrightarrow u_{7-i}$. (iii) The behaviors at the two endpoints are related by cycling $u_i\mapsto u_{i+1}$. (4) The final-entry (FE) condition.

MHV amplitudes obey a FE condition, which controls their first derivatives [40]. For $n=6$ and general kinematics, the FE condition removes three of the nine symbol letters [41], namely $1-u_i$, but at the origin these letters are irrelevant because they approach 1. Hence, the six-point FE condition trivializes at the origin.

In contrast, the seven-point FE condition allows 14 symbol letters for general kinematics [42], which collapse on LINE 71 to six letters out of a total of seven. We obtain a single constraint,

$$[u_7\partial_{u_7}+u_1\partial_{u_1}-u_4\partial_{u_4}]R_7=0, \tag{9}$$

where derivatives for $\ln u_7$ are taken independently of $\ln u_1$, despite the constraint $u_7+u_1=1$ on LINE 71. Combining

all constraints, the only allowed QL polynomials are exactly the three given in Eq. (7), and no linear-logarithmic structures survive. That is, the possible kinematic dependence of R_7 is already saturated by Eq. (7) at four loops. We will see that the TBA at strong coupling leads to precisely the same three $P_i^{(7)}$, and to a natural conjecture for all higher-loop corrections to the coefficients, which matches Eq. (8) through four loops.

The symbol of the eight-point remainder function R_8 is known at two and three loops [43,44]; it vanishes at all the origins and interpolating surfaces, as it must to be QL. For all the kinematics in Table II, we computed the full functions at two loops [45] and, in some cases, up to five loops using the pentagon operator product expansion (OPE) [6]. In all cases, we found that the remainder function R_8 is QL [47].

Furthermore, we repeated the all-loop seven-point analysis at eight points, starting on CUBE 6789, and then going on to other adjacent regions, using continuity at the boundaries between regions; see Fig. 1. In all cases, we found precisely five independent QL polynomials obeying the restrictions. On CUBE 6789, see Table II, they have the form,

$$R_8(\text{CUBE 6789}) = \sum_{i=1}^{5} d_i P_i^{(C)}, \tag{10}$$

where

$$P_1^{(C)} = \sum_{i=1}^{8} l_i^2 - 2\sum_{i=1}^{4} l_i l_{i+4} - 2(l_3 - l_7)(l_4 - l_8), \tag{11}$$

$$P_2^{(C)} = 2\sum_{i=1}^{4} l_i l_{i+4} + (l_3 - l_7)(l_4 - l_8) + (l_1 + l_5)(\ell_1 + \ell_4) + (l_3 + l_4 + l_7 + l_8)\ell_3 + (l_2 + l_6)\ell_2 + \sum_{i=1}^{4} \ell_i^2, \tag{12}$$

with $l_i \equiv \ln u_i$ and $\ell_i \equiv \ln v_i$. The lengthier $P_{3,4,5}^{(C)}$ are provided in Sec. D of the Supplemental Material [12]. One has $d_3 = d_4 = \zeta_2 g^4$ through two loops; the remaining coefficients start at higher orders. The same form, Eq. (10), applies in the other QL-connected regions, with the same d_i's but different polynomials. Similarly, the baby bootstrap yields a five-polynomial ansatz for SUPERLINE 1; since it is disconnected from the other regions, it comes with its own set of coefficients, f_i. We give the expressions for all five polynomials in all possible regions, along with weak coupling expansions of the d_i and f_i coefficients through eight loops, in the ancillary files `octagon_QL_formula.txt` and `octagon_QL_coefs.txt`.

Master formula from TBA.—Additional insight into the QL behavior of the amplitudes may be found at strong coupling using the AdS/CFT-dual string theory description, which maps the problem to computing the minimal world-sheet area for a string anchored on a null polygonal contour at the boundary of AdS [1]. Using the integrability of the classical string theory [48], it boils down to solving a set of nonlinear TBA integral equations [22,23]. We will now outline how the TBA equations can be linearized near origins. A (weighted) Fourier transformation from the TBA spectral parameter θ to a variable z, related to the tilt angle, converts the integral equations to a simple matrix equation, and allows us to express the minimal area (the logarithm of the strong-coupling amplitude) as a single integral over z. The crux of our finite-coupling conjecture is to move the 't Hooft coupling $\sqrt{\lambda}$ inside the integral and absorb it into the tilted cusp anomalous dimension. The resulting master formula, Eq. (20), can be evaluated either at finite coupling or at weak coupling where it agrees with all the perturbative data reviewed above.

For the TBA analysis, we use coordinates $\{\sigma_s, \tau_s, \varphi_s\}$, $s = 1, \ldots, n-5$, originally developed for analyzing the OPE [5,6]. The TBA equations are for a family of $3(n-5)$ functions $Y_{a,s}(\theta)$, with $a = \{0, \pm 1\}$ [5,24]

$$\ln Y_{a,s}(\theta) = I_{a,s}(\theta) + \sum_{b,t} \int \frac{k_a(\theta) d\theta'}{2\pi k_b(\theta')} K_{a,s}^{b,t}(\theta - \theta') \ln[1 + Y_{b,t}(\theta')], \tag{13}$$

where the sum runs over $b = 0, \pm 1$, $t = s$, $s \pm 1$, with $k_a(\theta) = i^a \sinh(2\theta - i\pi a/2)$ and for some kernels K. The driving terms $I_{a,s}$ encode the cross ratios, and are given explicitly in terms of the OPE coordinates,

$$I_{a,s}(\theta) = a\varphi_s - m_a \tau_s \cosh\theta + (-1)^s i m_a \sigma_s \sinh\theta, \tag{14}$$

with $m_a = 2\cos(a\pi/4)$. The dependence on the hyperbolic angle θ corresponds to a collection of interacting relativistic particles, of mass m_a and charge a, coupled to various temperatures $1/\tau_s$ and chemical potentials φ_s.

Drawing inspiration from the hexagon ($n = 6$) analysis [10,49], we expect origins to map to extreme limits where the particles are subject to large chemical potentials, $|\varphi_s| \to \infty$, and to small temperatures, $\tau_s \to \infty$. There are several ways of taking limits for $n > 6$. We may send each φ_s to either $+\infty$ or $-\infty$, with each case labeled by a sequence $\Sigma_n = (h_1, \ldots, h_{n-5})$ with $h_s = \varphi_s/|\varphi_s|$. In such limits, we expect the particles with $a = h_s$ to condense, and the remaining ones to decouple. Namely, for a given choice Σ_n, we assume that $Y_{a,s}(\theta) \gg 1$ if $a = h_s$ and $Y_{a,s} = 0$ otherwise, and linearize Eq. (13) using $\ln(1 + Y_{b,t}) \to \delta_{b,h_t} \ln Y_{h_t,t}$. We also assume that the above conditions hold over the entire real θ axis.

The problem may then be solved by going to Fourier space. One defines

$$\hat{f}(z) = \int_{-\infty}^{\infty} \frac{d\theta}{2\pi \cosh(2\theta)} z^{2i\theta/\pi} f(\theta), \tag{15}$$

with a measure introduced to eliminate the weight in Eq. (13) and with the Fourier variable $(2\ln z)/\pi$, with $z>0$, introduced to rationalize all expressions. Setting $Y_s = Y_{h_s,s}, I_s = I_{h_s,s}$, Eq. (13) yields

$$\widehat{\ln Y_s}(z) = \sum_{t=1}^{n-5} [1-K_n(z)]^{-1}_{s,t} \hat{I}_t(z), \tag{16}$$

with the square matrix $[K_n(z)]_{s,t} = \int (d\theta/2\pi) K^{h_t,t}_{h_s,s}(\theta) z^{2i\theta/\pi}$. At strong coupling, $\sqrt{\lambda} = 4\pi g \gg 1$, the remainder function is given by the TBA free energy [5,22,23], which becomes

$$R_n^{\text{string}} = -\frac{\sqrt{\lambda}}{\pi^2}\int_0^\infty \frac{dz}{z}\mathcal{S}_n(z) + \ldots, \tag{17}$$

$$\mathcal{S}_n(z) \equiv \sum_{s=1}^{n-5} \hat{I}_s(1/z)\widehat{\ln Y_s}(z). \tag{18}$$

The ellipses stand for a simple term $\propto \Gamma_{\text{cusp}}$, to which we shall return shortly. Importantly, the integrand $\mathcal{S}_n(z)$ is a rational function of z. For any limit Σ_n, it may be cast into the form (see Sec. E of the Supplemental Material [12] for details)

$$\mathcal{S}_n(z) = \frac{z(1-z^3)\mathcal{P}^\Sigma_n(z)}{(1+z)(1+z^2)[1-z^{3(n-4)}]}, \tag{19}$$

where $\mathcal{P}^\Sigma_n(z) = z^{3n-14}\mathcal{P}^\Sigma_n(1/z)$ is a polynomial of degree $3n-14$ in z and is quadratic in $\{\sigma_s,\tau_s,\varphi_s\}_{s=1,\ldots,n-5}$.

Equation (17) may be turned into an all-order conjecture by bringing $\sqrt{\lambda}$ under the integral sign and promoting it to a full function of the variable z. To be precise, we conjecture that R_n takes at finite coupling the form of a contour integral in the dual variable z,

$$R_n = -\frac{1}{2}\oint_{C_n}\frac{dz}{2\pi i z}(z-1/z)\tilde{\mathcal{G}}(z,g)\mathcal{S}_n(z), \tag{20}$$

with $\tilde{\mathcal{G}}(z,g) = \mathcal{G}(z,g) - \Gamma_{\text{cusp}}(g)$ and with $\mathcal{G}(z,g)$ the tilted cusp anomalous dimension, viewed here as a function of $z = -e^{2i\alpha}$,

$$\mathcal{G}(z,g) = \Gamma_\alpha(g). \tag{21}$$

Equation (20) neatly factorizes the coupling dependence, which resides in $\mathcal{G}(z,g)$, and the kinematics, which sits in the string integrand $\mathcal{S}_n(z)$. The contour C_n is a sum of small circles around the singularities of $\mathcal{S}_n(z)$; from Eq. (19) they are poles on the unit circle $|z|=1$, mapping to real angles α. The original string formula is recovered by using the strong-coupling behavior [10]

$$\Gamma_\alpha \approx \frac{2\alpha\sqrt{\lambda}}{\pi^2\sin(2\alpha)} \Rightarrow \mathcal{G}(z) \approx -\frac{2\sqrt{\lambda}\log(-z)}{\pi^2(z-1/z)}. \tag{22}$$

The integral in Eq. (17) follows from the term $\propto \mathcal{G}(z)$, by wrapping the contour on the logarithmic cut along $z>0$, whereas the term $\propto \Gamma_{\text{cusp}} = \Gamma_{\pi/4}$ accounts for the ellipses in Eq. (17).

At finite coupling, one may calculate Eq. (20) by residues, around the poles in Eq. (19), and write

$$R_n = \sum_\alpha \tilde{\Gamma}_\alpha(g) \times P^{\Sigma_n}_\alpha(\{\sigma_s,\tau_s,\varphi_s\}), \tag{23}$$

with $\tilde{\Gamma}_\alpha = \Gamma_\alpha - \Gamma_{\text{cusp}}$ and with the sum running over

$$\alpha = \frac{\pi}{2} - \frac{\pi p}{3} - \frac{\pi k}{3(n-4)}, \tag{24}$$

with $k = 1,\ldots,n-5$ and $p = 0,\ 1,\ 2$. The associated polynomials $P^{\Sigma_n}_\alpha$ follow straightforwardly from the TBA analysis, but are too bulky to be shown here (see Eq. (26) of the Supplemental Material [12]). At last, one may eliminate the OPE parameters in favor of the cross ratios, using general formulae in Ref. [50]. In the limit $|\varphi_s| \gg \tau_s \gg 1$, with σ_s held fixed, these relations reduce to simple mappings between the OPE parameters and the logarithms of the cross ratios.

For illustration, when $n=6$, one finds

$$u_1 \approx e^{\tau+\sigma-|\varphi|}, \qquad u_2 \approx e^{-2\tau}, \qquad u_3 \approx e^{\tau-\sigma-|\varphi|}, \tag{25}$$

and Eq. (23) and $P^{\Sigma_6}_\alpha$ give

$$R_6 = -\sum_{\alpha=0,\pm\pi/3}\frac{\tilde{\Gamma}_\alpha(g)}{24}|l_1 + e^{2i\alpha}l_2 + e^{4i\alpha}l_3|^2, \tag{26}$$

in perfect agreement with Ref. [10], using $\tilde{\Gamma}_{-\alpha} = \tilde{\Gamma}_\alpha$. For $n=7$, one gets

$$\begin{aligned} &u_1 \approx e^{\tau_2-\sigma_2-|\varphi_2|}, \quad u_2 \approx e^{-2\tau_2}, \quad u_3u_7 \approx e^{\tau_2+\sigma_2-|\varphi_2|}, \\ &u_6 \approx e^{\tau_1-\sigma_1-|\varphi_1|}, \quad u_5 \approx e^{-2\tau_1}, \quad u_4u_7 \approx e^{\tau_1+\sigma_1-|\varphi_1|}, \end{aligned} \tag{27}$$

with $u_7 = 1$ for $\Sigma_7 = (+,+)$, and $u_3+u_4=1$ for $\Sigma_7 = (+,-)$, corresponding, respectively, to the origin $O_7^{(7)}$ and a cyclic image of LINE 71. Using $P^{\Sigma_7}_\alpha$, we find a perfect agreement with the general decomposition for the heptagon line, Eq. (6), with $c_3 = a_3 - a_1/2, c_2 = -a_3$, $c_1 = a_2 - a_1/2$, where

$$a_j = \frac{(-1)^j}{3\sqrt{3}}\sum_{k=1}^{3}(-1)^k \sin(2\alpha_k)\cos(2(j-1)\alpha_k)\tilde{\Gamma}_{\alpha_k}(g), \tag{28}$$

and $\alpha_{1,2,3} = \{\pi/18, 5\pi/18, 7\pi/18\}$. The coefficients agree with the perturbative results, Eq. (8), taking into account the weak-coupling expansion of the tilted cusp anomalous dimension [10], $\Gamma_\alpha(g) = 4g^2 - 16\zeta_2 g^4\cos^2\alpha + O(g^6)$, as discussed further in Sec. A of the Supplemental Material [12].

One may proceed similarly for $n=8$ using $\Sigma_8 = (+,+,+),(+,+,-),(+,-,+)$ and find three domains describing, respectively, the origin O_9, a line $O_3 - O_4$, and a square ending on O_8, O_9, and two images of O_7. In all of these cases, we found perfect agreement with the

perturbative results, with the coefficients matching the two-loop predictions and the five-loop OPE results.

This analysis does not exhaust all the origins and domains given in Table II. For example, for (an image of) CUBE 6789 it covers but a single face. To reach the missing domains, one should look at a broader class of scalings, where not only φ_s and τ_s are allowed to be large but also σ_s. These scalings are harder to address in general because the limit $|\sigma_s| \to \infty$ generates large fluctuations in the Y functions, making it hard to decide which of them are large and which are small. It may also trigger new exceptional solutions, with more particle species condensing simultaneously. In Sec. F of the Supplemental Material [12], we argue that this happens at $n = 8$ for SUPERLINE 1; we conjecture that its QL behavior is captured by a system of linearized TBA equations based on four large Y functions.

Conclusions.—In this Letter, we initiated a systematic exploration of origins: kinematical points and interpolating higher-dimensional surfaces where high-multiplicity MHV scattering amplitudes in planar $\mathcal{N} = 4$ SYM simplify dramatically and can be predicted (conjecturally) at finite coupling. Cluster algebras provide a road map to the kinematics, while the TBA and the tilted cusp anomalous dimension $\Gamma_\alpha(g)$ both play a central role in the master formula for the leading singular behavior. We expect further kinematical richness to emerge for $n > 8$, based on the appearance of the super-origin O_1 at $n = 8$, which is not connected (by any QL lines) to the other eight-point origins. We also have not ruled out the possibilities of even more kinematic boundaries of the positive region with QL behavior, especially for $n \geq 8$. The behavior in all these regions will certainly play a key role in constraining the all-orders behavior of MHV amplitudes for generic kinematics. Our findings may also have implications for other planar $\mathcal{N} = 4$ observables, such as correlators of large-charge operators, which exhibit QL behavior for small cross ratios [51–54]. The great similarity between the two problems suggests that a similar origin story, with a rich pattern of limits and tilted cusp anomalous dimensions, may be uncovered for all these higher-point functions.

We are grateful to Niklas Henke, Gab Dian, Andrew McLeod, Amit Sever, and Pedro Vieira for interesting discussions. The work of B. B. was supported by the French National Agency for Research Grant No. ANR-17-CE31-0001-02. The work of L. D. and Y. L. was supported by the US Department of Energy under Contract No. DE–AC02–76SF00515. Y. L. was also supported in part by the Benchmark Stanford Graduate Fellowship, the Heising-Simons Foundation, the Simons Foundation, and National Science Foundation Grant No. NSF PHY-1748958. G. P. acknowledges support from the Deutsche Forschungsgemeinschaft under Germany's Excellence Strategy—EXC 2121 "Quantum Universe"—390833306. B. B., Y. L., and L. D. thank the Kavli Institute for Theoretical Physics for hospitality.

*Corresponding author.
benjamin.basso@phys.ens.fr
†Corresponding author.
lance@slac.stanford.edu
‡Corresponding author.
aytliu@stanford.edu
§Corresponding author.
georgios.papathanasiou@desy.de

[1] L. F. Alday and J. M. Maldacena, Gluon scattering amplitudes at strong coupling, J. High Energy Phys. 06 (2007) 064.
[2] J. M. Drummond, G. P. Korchemsky, and E. Sokatchev, Conformal properties of four-gluon planar amplitudes and Wilson loops, Nucl. Phys. **B795**, 385 (2008).
[3] A. Brandhuber, P. Heslop, and G. Travaglini, MHV amplitudes in $N = 4$ super Yang-Mills and Wilson loops, Nucl. Phys. **B794**, 231 (2008).
[4] J. M. Drummond, J. Henn, G. P. Korchemsky, and E. Sokatchev, Conformal ward identities for Wilson loops and a test of the duality with gluon amplitudes, Nucl. Phys. **B826**, 337 (2010).
[5] L. F. Alday, D. Gaiotto, J. Maldacena, A. Sever, and P. Vieira, An operator product expansion for polygonal null Wilson loops, J. High Energy Phys. 04 (2011) 088.
[6] B. Basso, A. Sever, and P. Vieira, Spacetime and Flux Tube S-Matrices at Finite Coupling for $N = 4$ Supersymmetric Yang-Mills Theory, Phys. Rev. Lett. **111**, 091602 (2013).
[7] S. S. Gubser, I. R. Klebanov, and A. M. Polyakov, A Semi-classical limit of the gauge/string correspondence, Nucl. Phys. **B636**, 99 (2002).
[8] L. F. Alday and J. M. Maldacena, Comments on operators with large spin, J. High Energy Phys. 11 (2007) 019.
[9] S. Caron-Huot, L. J. Dixon, F. Dulat, M. von Hippel, A. J. McLeod, and G. Papathanasiou, Six-Gluon amplitudes in planar $\mathcal{N} = 4$ super-Yang-Mills theory at six and seven loops, J. High Energy Phys. 08 (2019) 016.
[10] B. Basso, L. J. Dixon, and G. Papathanasiou, Origin of the Six-Gluon Amplitude in Planar $N = 4$ Supersymmetric Yang-Mills Theory, Phys. Rev. Lett. **124**, 161603 (2020).
[11] N. Beisert, B. Eden, and M. Staudacher, Transcendentality and crossing, J. Stat. Mech. (2007) P01021.
[12] See Supplemental Material at http://link.aps.org/supplemental/10.1103/PhysRevLett.130.111602 for details on the tilted cusp anomalous dimension, Gram determinant constraints, cluster algebras, TBA analysis, and the octagon kinematics for CUBE 6789 and SUPERLINE 1, which includes Refs. [13–15].
[13] M. K. Benna, S. Benvenuti, I. R. Klebanov, and A. Scardicchio, A Test of the AdS/CFT Correspondence using High-Spin Operators, Phys. Rev. Lett. **98**, 131603 (2007).
[14] A. Hodges, Eliminating spurious poles from gauge-theoretic amplitudes, J. High Energy Phys. 05 (2013) 135.
[15] V. Del Duca, S. Druc, J. Drummond, C. Duhr, F. Dulat, R. Marzucca, G. Papathanasiou, and B. Verbeek, Multi-Regge kinematics and the moduli space of Riemann spheres with marked points, J. High Energy Phys. 08 (2016) 152.
[16] S. Fomin and A. Zelevinsky, Cluster algebras I: Foundations, J. Am. Math. Soc. **15**, 497 (2002).
[17] S. Fomin and A. Zelevinsky, Cluster algebras II: Finite type classification, Invent. Math. **154**, 63 (2003).

[18] V. V. Fock and A. B. Goncharov, Cluster ensembles, quantization and the dilogarithm, Ann. Sci. Éc. Norm. Supér. **42**, 865 (2009).

[19] N. Arkani-Hamed, J. L. Bourjaily, F. Cachazo, A. B. Goncharov, A. Postnikov, and J. Trnka, *Grassmannian Geometry of Scattering Amplitudes* (Cambridge University Press, Cambridge, England, 2016), 10.1017/CBO9781316091548.

[20] J. Golden, A. B. Goncharov, M. Spradlin, C. Vergu, and A. Volovich, Motivic amplitudes and cluster coordinates, J. High Energy Phys. 01 (2014) 091.

[21] V. V. Fock and A. B. Goncharov, Cluster poisson varieties at infinity, Sel. Math. **22**, 2569 (2016).

[22] L. F. Alday, D. Gaiotto, and J. Maldacena, Thermodynamic bubble ansatz, J. High Energy Phys. 09 (2011) 032.

[23] L. F. Alday, J. Maldacena, A. Sever, and P. Vieira, Y-system for scattering amplitudes, J. Phys. A **43**, 485401 (2010).

[24] A. Bonini, D. Fioravanti, S. Piscaglia, and M. Rossi, Strong Wilson polygons from the lodge of free and bound mesons, J. High Energy Phys. 04 (2016) 029.

[25] J. Drummond, J. Henn, V. Smirnov, and E. Sokatchev, Magic identities for conformal four-point integrals, J. High Energy Phys. 01 (2007) 064.

[26] N. Arkani-Hamed, T. Lam, and M. Spradlin, Non-perturbative geometries for planar $\mathcal{N} = 4$ SYM amplitudes, J. High Energy Phys. 03 (2021) 065.

[27] J. S. Scott, Grassmannians and cluster algebras, arXiv:math/0311148.

[28] G. Papathanasiou, The SAGEX review on scattering amplitudes, Chapter 5: Analytic bootstraps for scattering amplitudes and beyond, J. Phys. A **55**, 443006 (2022).

[29] J. Drummond, J. Foster, Ö. Gürdoğan, and C. Kalousios, Tropical Grassmannians, cluster algebras and scattering amplitudes, J. High Energy Phys. 04 (2020) 146.

[30] J. Drummond, J. Foster, Ö. Gürdoğan, and C. Kalousios, Algebraic singularities of scattering amplitudes from tropical geometry, J. High Energy Phys. 04 (2021) 002.

[31] N. Henke and G. Papathanasiou, How tropical are seven- and eight-particle amplitudes?, J. High Energy Phys. 08 (2020) 005.

[32] N. Henke and G. Papathanasiou, Singularities of eight- and nine-particle amplitudes from cluster algebras and tropical geometry, J. High Energy Phys. 10 (2021) 007.

[33] D. Speyer and L. Williams, The tropical totally positive Grassmannian, J. Algebraic Comb. **22**, 189 (2005).

[34] N. Arkani-Hamed, S. He, and T. Lam, Stringy canonical forms, J. High Energy Phys. 02 (2021) 069.

[35] The A_3 polytope is a truncated triangular bipyramid, but if we collapse its vertices that correspond to the same points in cross-ratio space, we get a cube in both cases.

[36] Z. Bern, L. J. Dixon, and V. A. Smirnov, Iteration of planar amplitudes in maximally supersymmetric Yang-Mills theory at three loops and beyond, Phys. Rev. D **72**, 085001 (2005).

[37] Z. Bern, L. J. Dixon, D. A. Kosower, R. Roiban, M. Spradlin, C. Vergu, and A. Volovich, The two-loop six-gluon MHV amplitude in maximally supersymmetric Yang-Mills theory, Phys. Rev. D **78**, 045007 (2008).

[38] J. M. Drummond, J. Henn, G. P. Korchemsky, and E. Sokatchev, Hexagon Wilson loop = six-gluon MHV amplitude, Nucl. Phys. **B815**, 142 (2009).

[39] L. J. Dixon and Y.-T. Liu, Lifting Heptagon symbols to functions, J. High Energy Phys. 10 (2020) 031.

[40] S. Caron-Huot and S. He, Jumpstarting the all-loop S-matrix of planar $N = 4$ super Yang-Mills, J. High Energy Phys. 07 (2012) 174.

[41] A. B. Goncharov, M. Spradlin, C. Vergu, and A. Volovich, Classical Polylogarithms for Amplitudes and Wilson Loops, Phys. Rev. Lett. **105**, 151605 (2010).

[42] J. M. Drummond, G. Papathanasiou, and M. Spradlin, A symbol of uniqueness: The cluster bootstrap for the 3-loop MHV heptagon, J. High Energy Phys. 03 (2015) 072.

[43] S. Caron-Huot, Superconformal symmetry and two-loop amplitudes in planar $N = 4$ super Yang-Mills, J. High Energy Phys. 12 (2011) 066.

[44] Z. Li and C. Zhang, The three-loop MHV octagon from $\bar{Q}$ equations, J. High Energy Phys. 12 (2021) 113.

[45] We thank A. McLeod for confirming one of these limits using results in Ref. [46].

[46] J. Golden and A. J. McLeod, The two-loop remainder function for eight and nine particles, J. High Energy Phys. 06 (2021) 142.

[47] We have checked that the full one-loop amplitude, including all non-dual-conformal terms associated with infrared divergences, is QL for all $n = 6, 7, 8$ origins. This suffices to show that the logarithm of the full amplitude is QL. The nontrivial statement is that the dilogarithms of generic arguments cancel out, which requires the use of the five-term dilog identity for PENTAGONS 234 and 345.

[48] I. Bena, J. Polchinski, and R. Roiban, Hidden symmetries of the AdS_5 x S^5 superstring, Phys. Rev. D **69**, 046002 (2004).

[49] K. Ito, Y. Satoh, and J. Suzuki, MHV amplitudes at strong coupling and linearized TBA equations, J. High Energy Phys. 08 (2018) 002.

[50] B. Basso, A. Sever, and P. Vieira, Space-time S-matrix and flux tube S-matrix II. Extracting and matching data, J. High Energy Phys. 01 (2014) 008.

[51] F. Coronado, Bootstrapping the Simplest Correlator in Planar $\mathcal{N} = 4$ SYM at All Loops, Phys. Rev. Lett. **124**, 171601 (2020).

[52] I. Kostov, V. B. Petkova, and D. Serban, The octagon as a determinant, J. High Energy Phys. 11 (2019) 178.

[53] A. V. Belitsky and G. P. Korchemsky, Exact null octagon, J. High Energy Phys. 05 (2020) 070.

[54] C. Bercini, V. Gonçalves, and P. Vieira, Light-Cone Bootstrap of Higher Point Functions and Wilson Loop Duality, Phys. Rev. Lett. **126**, 121603 (2021).